

## Report

# Estrogen-Induced Rat Breast Carcinogenesis is Characterized by Alterations in DNA Methylation, Histone Modifications and Aberrant MicroRNA Expression

Olga Kovalchuk<sup>1,\*</sup>

Volodymyr P. Tryndyak<sup>2</sup>

Beverly Montgomery<sup>2</sup>

Alex Boyko<sup>1</sup>

Kristy Kutanzi<sup>1</sup>

Franz Zemp<sup>1</sup>

Alan R. Warbritton<sup>3</sup>

John R. Latendresse<sup>3</sup>

Igor Kovalchuk<sup>1</sup>

Frederick A. Beland<sup>2</sup>

Igor P. Pogribny<sup>2,\*</sup>

<sup>1</sup>Department of Biological Sciences; University of Lethbridge; Lethbridge, Canada

<sup>2</sup>Division of Biochemical Toxicology; National Center for Toxicological Research; Jefferson, Arizona USA

<sup>3</sup>Toxicologic Pathology Associates; National Center for Toxicological Research; Jefferson, Arizona USA

\*Correspondence to: Igor P. Pogribny; Division of Biochemical Toxicology; National Center for Toxicological Research; Jefferson, Arizona 72079 USA; Tel.: 870.543.7096; Fax: 870.543.7720; Email: igor.pogribny@fda.hhs.gov/Olga Kovalchuk; Department of Biological Sciences; University of Lethbridge; Lethbridge AB T1K 3M4 Canada; Tel.: +403.394.3916; Fax: 403.329.2242; Email: olga.kovalchuk@uleth.ca

Original manuscript submitted: 06/05/07  
Manuscript accepted: 06/06/07

Previously published online as a *Cell Cycle* E-publication:  
<http://www.landesbioscience.com/journals/cc/articles/4549>

## KEY WORDS

<sup>17</sup> $\beta$ -estradiol, breast carcinogenesis, rat, DNA methylation, histone methylation, microRNA

## ACKNOWLEDGEMENTS

This work was supported in part by a Postgraduate Research Program administered by the Oak Ridge Institute for Science and Education (V.P.T.) and by Alberta Breast Cancer Initiative grant (O.K.).

## ABSTRACT

Breast cancer is the most common malignancy in women continuing to rise worldwide. Breast cancer emerges through a multi-step process, encompassing progressive changes from a normal cell to hyperplasia (with and without atypia), carcinoma in situ, invasive carcinoma, and metastasis. In the current study, we analyzed the morphological changes and alterations of DNA methylation, histone methylation and microRNA expression during estradiol-17 $\beta$  (E<sub>2</sub>)-induced mammary carcinogenesis in female August Copenhagen Irish (ACI) rats. E<sub>2</sub>-induced breast carcinogenesis in ACI rats provides a physiologically relevant and genetically defined animal model for studying human sporadic breast cancer. The pattern of morphological changes in mammary glands during E<sub>2</sub>-induced carcinogenesis was characterized by transition from normal appearing alveolar and ductular hyperplasia to focal hyperplastic areas of atypical glands and ducts accompanied by a rapid and sustained loss of global DNA methylation, LINE-1 hypomethylation, loss of histone H3 lysine 9 and histone H4 lysine 20 trimethylation, and altered microRNAs expression. More importantly, these alterations in the mammary tissue occurred after six weeks of E<sub>2</sub>-treatment, whereas the atypical hyperplasia, which represents a putative precursor lesion to mammary carcinoma in this model, was detected only after twelve weeks of exposure, demonstrating clearly that these events are directly associated with the effects of E<sub>2</sub> and are not a consequence of the preexisting preneoplastic lesions. The results of this study show that deregulation of cellular epigenetic processes plays a crucial role in the mechanism of E<sub>2</sub>-induced mammary carcinogenesis in ACI rats, especially in the tumor initiation process.

## INTRODUCTION

Breast cancer is the most common malignancy in women. It is the second leading cause of cancer deaths among North American women, and the leading cause of death among women aged 35 to 55 years.<sup>1,2</sup> Furthermore, the worldwide incidence of breast cancer is continuing to rise.<sup>2</sup>

Breast cancer emerges through a multi-step process, encompassing progressive changes from a normal cell to hyperplasia (with and without atypia), carcinoma in situ, invasive carcinoma, and metastasis.<sup>3,4</sup> Presently, cancer, including breast cancer, is recognized as both a genetic and epigenetic disease.<sup>5-7</sup> "Genetic" is defined as an heritable change in the DNA sequence, while "epigenetic" refers to the information contained in chromatin rather than in the actual DNA sequence.<sup>5</sup> Epigenetic changes broadly encompass alterations in DNA methylation, histone modifications, and changes induced by non-coding small RNAs.<sup>5</sup> While the sequential accumulation of various genetic changes in the genesis of breast cancer has been extensively studied,<sup>3,4</sup> the contributions of epigenetic alterations to the etiology of breast cancer have not been elucidated.

In recent years the role of epigenetics in the molecular etiology of cancer has been increasingly recognized.<sup>5-8</sup> A change in cytosine DNA methylation was the first identified epigenetic alteration in cancer and is the best-studied epigenetic mechanism thus far.<sup>9-11</sup> Two types of changes in the DNA methylation pattern occur in cancer: regional DNA hypermethylation and global and regional DNA hypomethylation.<sup>7,8</sup> Until now, most of the research in the field of cancer epigenetics has been focused on the role of an increased methylation status of the specific gene promoters responsible for initiating or enforcing the silencing of tumor suppressor genes.<sup>8,12</sup> In contrast, DNA hypomethylation, although the first epigenetic abnormality identified in cancer,<sup>9-11</sup> has received much less attention. Recent studies have provided evidence of an association between a decrease in global or

regional DNA methylation and the progression of advanced and metastatic breast cancer,<sup>13-15</sup> however, very little is known about the role of altered DNA methylation in breast cancer predisposition and etiology.

DNA methylation is closely connected with other components of chromatin, primarily histone modifications.<sup>16</sup> Despite the fact that recent studies have shown importance of aberrant histone modifications in cancer,<sup>17-19</sup> no profile of overall histone modification changes during breast carcinogenesis has been described.

Recently, much attention has been given to the silencing of genes through the action of small RNAs. The key regulators of this novel phenomenon are 21–25 nucleotide-long microRNAs (miRNAs). miRNAs are presently recognized as major regulators of gene expression<sup>20,21</sup> and various epigenetic processes.<sup>22</sup> Alternatively, some miRNAs are controlled by epigenetic mechanisms.<sup>23,24</sup> Aberrant levels of miRNAs have been reported in a variety of human cancers,<sup>25,26</sup> including breast cancer,<sup>27</sup> however the dynamics of miRNA changes during pre-malignant stages have not been studied.

Overall, there exists a major gap in the understanding of the role of epigenetic dysregulation in breast cancer development and progression, especially a lack of knowledge of how specific epigenetic changes may be mechanistically related to neoplastic transformation, and the precise timeline of epigenetic alterations occurring between the transitions of a normal cell through intermediate tumorigenic stages to a tumor cell.<sup>28,29</sup> Investigating the molecular mechanisms of this multistep process in humans is frequently impractical and, in most cases, unethical.<sup>30</sup> In contrast, relevant animal models of mammary gland carcinogenesis provide a unique opportunity for the study of breast cancer initiation.

Considering the results of recent epidemiological studies showing a causative role of estrogen in human breast cancer development,<sup>31,32</sup> especially in pre-menopausal women,<sup>31</sup> and the fact that estrogen-induced mammary gland tumorigenesis in female ACI rats is remarkably similar to human breast cancer,<sup>33,34</sup> the present study was undertaken to investigate the role of epigenetic changes in the etiology of estrogen-induced breast cancer.

## METHODS

**Animals, treatment and tissue preparations.** Intact, female ACI rats were purchased from Harlan Sprague-Dawley, Inc. (Indianapolis, IN). The animals were housed two per cage in a temperature-controlled (24°C) room with a 12 hour light-dark cycle, and given ad libitum access to water and NIH-31 pellet diet. At eight weeks of age, the rats were allocated randomly into two groups of twenty rats each. Group 1 received no treatment (control group). Group 2 received a single pellet containing 25 mg of 90-day release 17 $\beta$ -estradiol (E<sub>2</sub>). The pellets (Innovative Research of America, Sarasota, FL) were surgically implanted in the shoulder region.<sup>31,32</sup> Five rats per group were humanely euthanized using an overdose of CO<sub>2</sub> after 6, 12, and 18 weeks of treatment. All animal experimental procedures were carried out in accordance with animal study protocols approved by the National Center for Toxicological Research Animal Care and Use Committee.

The paired caudal inguinal mammary glands (and fat pad) were quickly excised. One gland was frozen immediately in liquid nitrogen and stored at -80°C for subsequent analyses. The contralateral gland and fat pad were carefully spread onto a 5 x 8 cm glass slide and observed grossly by transluminescence, allowing the orientation of the ducts and alveolar lobules to be visualized. The excess fat and

other tissue was trimmed. The gland was then carefully removed from the slide and placed into a cassette so the gland was oriented in a frontal (coronal) plane. This orientation demonstrated the arborizing pattern of the duct system and associated alveoli more clearly than could be obtained using a transverse section of the gland. The specimens were then fixed in 10% neutral buffered formalin for 48 h, processed, embedded in paraffin, sectioned at 4 microns, and mounted on glass slides. The sections were stained with hematoxylin and eosin for histopathological examination.

**Global DNA methylation analysis.** The extent of the global DNA methylation was evaluated with a radiolabeled [<sup>3</sup>H]-dCTP extension assay as described previously.<sup>35</sup>

**Methylation analysis of long interspersed nucleotide elements (LINE-1).** Methylation status of LINE-1 was determined by the COBRA assay, which consists of a standard bisulfite modification of genomic DNA, subsequent PCR amplification and digestion of the PCR product with the appropriate restriction endonuclease as previously described in detail.<sup>36</sup>

**Histone extraction.** Acidic cell extracts were prepared from frozen mammary tissue samples using a lysis buffer containing 10 mM HEPES (pH 7.9), 1.5 mM MgCl<sub>2</sub>, 10 mM KCl, 500  $\mu$ M DTT, 1.5 mM PMSF, followed by addition of HCl to a final concentration of 200 mM according to manufacturer's protocol (Upstate, Charlottesville, VA). Cell lysates were centrifuged at 14,000 x g for 10 min at 4°C, and the acid-insoluble pellets were discarded. The supernatant fractions, which contain the acid-soluble proteins, were purified by sequential dialysis against 100 mM acetic acid, then H<sub>2</sub>O. Protein concentrations were determined by the Bradford assay and aliquots of total histones were stored at -80°C.

**Analysis of histone modifications.** Equal amount of total histones (40  $\mu$ g) were mixed with two volumes of gel loading buffer (250 mM Tris-HCl (pH 8.0), 20%  $\beta$ -mercaptoethanol, 40% glycerol, 8% SDS, 1.2 mg/ml bromophenol blue), heated for 5 min at 95°C, and resolved on 15% polyacrylamide gels. Proteins were transferred onto PVDF membranes. The membranes were blocked for 4 h in Tris-buffered saline (TBS) containing 5% nonfat dry milk and 0.1% Tween-20. Anti-trimethyl-histone H3 lysine 9 (1:1000; Upstate), anti-trimethyl-histone H4 lysine20 (1:2000; Upstate), anti-histone H3 (1:1000; Upstate), and anti-histone H4 (1:1000; Upstate) primary antibodies were diluted and used according to manufacturer's recommendations. Primary antibody binding was performed at 4°C overnight with constant shaking. A secondary donkey anti-rabbit antibody, labeled with alkaline phosphatase (Santa Cruz Biotechnology, Santa Cruz, CA), was applied at 1:5000 dilutions and binding was carried out at room temperature for 1.5 h. Chemifluorescence detection was performed with the ECF Substrate for Western Blotting (GE Healthcare, Piscataway, NJ) and measured directly by Storm Imaging System (Molecular Dynamics). Images are representative of three independent immunoblots and were analyzed by ImageQuant software. All membranes were stained with Coomassie Blue to confirm equal protein loading.

**Western blot analysis of protein expression.** Mammary tissue lysates were prepared by homogenization of 50 mg of tissue in 500  $\mu$ l of lysis buffer (50 mM Tris-HCl, pH 7.4; 1% NP-40; 0.25% sodium deoxycholate; 150 mM NaCl; 1 mM EDTA; 1 mM PMSF; 1  $\mu$ g/ml each aprotinin, leupeptin, pepstatin; 1 mM Na<sub>3</sub>VO<sub>4</sub>; 1 mM NaF), sonication, and incubation at 4°C for 30 min, followed by centrifugation at 10,000 x g at 4°C for 20 min. Extracts containing equal quantities of proteins were separated by SDS-PAGE on 10% polyacrylamide gels and transferred to PVDF membranes. Membranes

were probed with primary antibodies against Suv39h1 (1:1000; Upstate) and Suv4-20h2 (1:1500; Abcam, Cambridge, MA) histone methyltransferase, DNA methyltransferase 1 (DNMT1) (1:1000; Abcam), Aurora-A kinase (L-18, 1:100; Santa Cruz Biotechnology), BCL6 (1:200, Santa Cruz Biotechnology), c-Myc (1:300, Santa Cruz Biotechnology), E2F1 (1:500, Labvision Neomarkers, Fremont, CA) and RB1 (1:750, Labvision Neomarkers). Alkaline phosphatase-coupled donkey anti-rabbit secondary antibodies were used for visualization.

**miRNA microarray expression analysis.** Total RNA was extracted from rat liver tissues using TRIzol Reagent (Invitrogen, Burlington, Ontario) according to the manufacturer's instructions. miRNA microarray analysis was performed by LC Sciences (Houston, TX). Ten micrograms of total RNA were size-fractionated (<200 nucleotides) by using a *mirVana* kit (Ambion, Austin, TX). Poly-A tails were added to the RNA sequences at the 3' ends using a poly(A) polymerase, and nucleotide tags were then ligated to the poly-A tails. The tagged RNAs were hybridized to the dual-channel microarray  $\mu$ ParaFlo microfluidics chips (LC Sciences) containing 439 miRNA probes to rat and mouse miRNAs and then labeled with tag-specific dendrimer Cy3 and Cy5 fluorescent dyes. Dye switching was performed to eliminate the dye bias. The melting temperature of the detection probes was balanced by incorporation of varying numbers of modified nucleotides with increased binding affinities. Hybridization images were collected using a GenePix 4000B laser scanner (Molecular Devices, Sunnyvale, CA) and digitized using Array-Pro image analysis software (Media Cybernetics, Silver Spring, MD). The maximum signal level of background probes was 180. A miRNA detection signal threshold was defined as twice the maximum background signal. Normalization was performed with a cyclic LOWESS (locally-weighted regression) method to remove system-related variations.<sup>37</sup> Data adjustments included data-filtering, log<sub>2</sub> transformation, and gene centering and normalization. t-test analysis was conducted between control and E<sub>2</sub>-treated sample groups. miRNAs with p values < 0.05 were selected for cluster analysis. The clustering analysis was performed with a hierarchical method and with average linkage and Euclidean distance metrics.<sup>38</sup>

**Quantitative RT-PCR (qRT-PCR) expression analysis.** qRT-PCRs were performed by using SuperTaq Polymerase (Ambion) and a *mirVana* qRT-PCR miRNA Detection Kit (Ambion) following the manufacturer's instructions. Reactions contained *mirVana* qRT-PCR Primer Sets specific for miR-17-5p, miR-20a, miR-21, miR-22, miR-92, miR-106a, miR-127 and miR-129-3p; human 5S rRNA served as the positive control. qRT-PCR was performed on a SmartCycler (Cepheid, Sunnyvale, CA) and end-point reaction products were also analyzed on a 3.5% high-resolution agarose gel stained with ethidium bromide. The results are presented as the fold change of each miRNA normalized to that of 5S rRNA in mammary glands of E<sub>2</sub>-treated rats relative to control rats.

**Statistical analysis.** Results are presented as mean  $\pm$  S.E.M. Statistical analyses were conducted by two-way ANOVA, using treatment and weeks as fixed factors, with pair-wise comparisons being conducted by the Student-Newman-Keuls test. p-Values <0.05 were considered significant.

## RESULTS

**Morphological changes during estrogen-induced mammary carcinogenesis.** Exposure of ACI female rats to a constant elevated level of E<sub>2</sub> produced significant temporal histopathologic changes

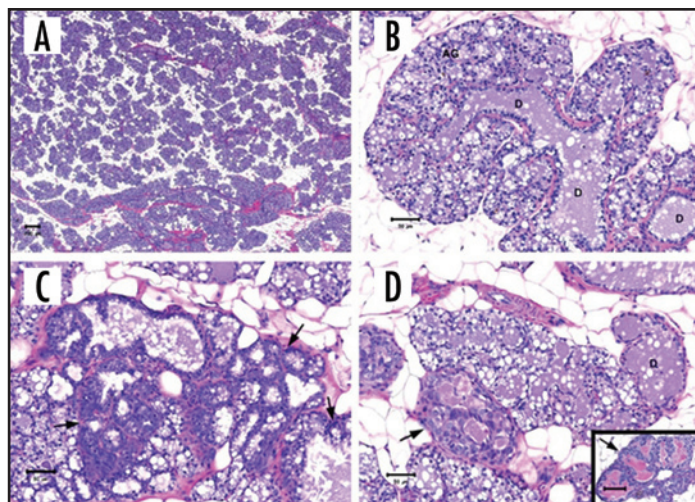


Figure 1. Histomorphological changes in mammary gland of female ACI rats exposed to E<sub>2</sub>. (A) Lobular hyperplasia, mammary gland, 6 weeks (25x). (B) Lobular hyperplasia, mammary gland, 12 weeks. Lobule with typical (normal appearing) intralobular ducts (D) and alveolar glands (AG) (200x). (C) Atypical alveolar hyperplasia (arrows), mammary gland, 12 weeks. Basophilic cytoplasm suggests increased RNA compared to typical alveolar hyperplasia (200x). (D) Atypical ductal hyperplasia (arrow), mammary gland, 18 weeks. Insert: atypical ductal hyperplasia. Epithelial papillary folds and stratification and eosinophilic secretion into lumen (200x). Sections (A–D) stained with hematoxylin and eosin.

(Fig. 1). E<sub>2</sub>-induced lobular hyperplasia of the mammary gland progressed from six weeks to twelve weeks of exposure. The lobular hyperplasia was characterized as an increase in the number and size of normal appearing alveoli and ducts per unit area of tissue (Fig. 1A). Typical or normal appearing intralobular ducts and ductules were also components of this hyperplasia (Fig. 1B). The secretory epithelium of alveoli was well differentiated and consisted of a single layer. Variability in alveolar and cellular size appeared to be due to the secretory activity and the number of cytoplasmic lipid vacuoles. The intralobular ducts were lined by a single layer of low cuboidal epithelium with a low cytoplasmic to nuclear ratio (Fig. 1B).

Between 6 and 12 weeks of exposure, atypical hyperplasia of both ducts and alveoli developed. The atypical hyperplastic alveolar foci manifested a distinctly different morphology than normal appearing alveoli. In these foci, the alveolar lumens were sometimes slightly enlarged and irregularly shaped (Fig. 1C). The secretory epithelium was only occasionally stratified, having two to three layers. The alveolar epithelial cells and their nuclei were variable in size, often larger than those in normally appearing secretory cells in adjacent typical normally appearing alveoli. The cytoplasm was distinctly more basophilic and nuclear membranes and nucleoli were prominent. Numerous large vacuoles at the apical edge of the cells gave the luminal margin a serrated contour. After 18 weeks of E<sub>2</sub> exposure, small and intermediate sized ducts were either clustered together forming separate distinct foci or nestled between normal appearing alveolar glands (Fig. 1D). The intermediate and larger ducts were sometimes lined by stratified and/or papillary fronds of proliferated epithelium (Fig. 1D insert). The smaller ducts or ductules were usually lined by a single layer of epithelial cells morphologically similar to the larger and intermediate sized ducts. The ductal lumens were commonly filled with a deeply eosinophilic secretion (Fig. 1D insert). The epithelial cells of these atypical ducts were often signifi-

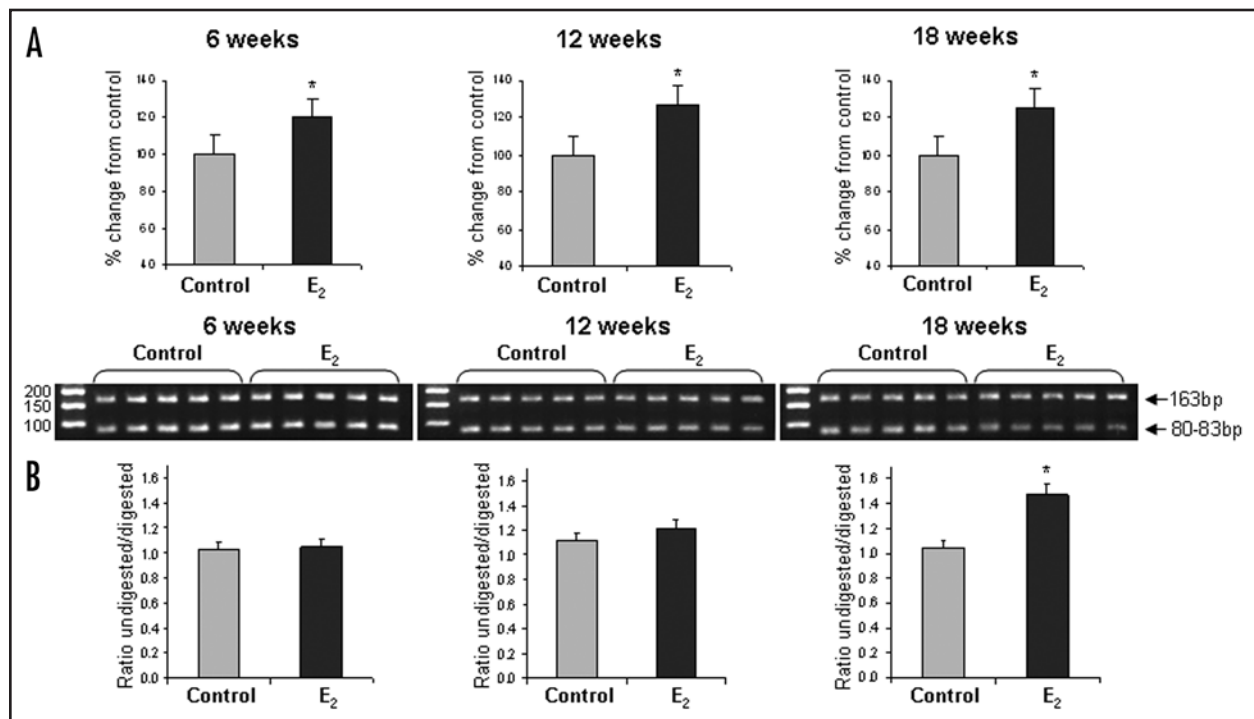


Figure 2. Level of DNA methylation and expression of DNA methyltransferase 1 in mammary glands of control rats and rats exposed to E<sub>2</sub>. (A) Status of global DNA methylation in the mammary glands of control and E<sub>2</sub>-exposed female ACI rats. DNA methylation was measured by a cytosine extension assay after treatment of DNA with methylation-sensitive restriction endonuclease HpaII, which cleaves CCGG sequences when internal cytosine residues are unmethylated on both strands. (B) Methylation status of LINE-1 in the mammary glands of control and E<sub>2</sub>-exposed ACI rats as detected by the COBRA assay. The upper panel shows representative photographs of the COBRA assay with the BstUI restriction endonuclease. The lower panel shows quantitative analysis of ratio between uncut (163 bp) and BstUI-cut (80–83 bp) PCR products in the mammary glands of E<sub>2</sub>-exposed rats and the age-matched control rats. The increased ratio between undigested and BstUI-digested PCR products in E<sub>2</sub>-exposed rats indicates the loss of LINE-1 methylation because cleavage of PCR products would occur only if the CpG dinucleotides within BstUI recognition sequence (CGCG) are methylated. (C) Expression of DNMT1 in the mammary glands of control and E<sub>2</sub>-exposed female ACI rats. Mammary tissue lysates were separated by SDS-PAGE and subjected to Western immunoblotting using specific antibodies against DNMT1 and PCNA. Equal sample loading was confirmed by immunostaining against  $\beta$ -actin. These results were reproduced in two independent experiments. Representative Western immunoblot images are shown. The lower panel shows quantitative analysis of DNMT1 protein level normalized to PCNA level. Data are presented as relative to age-matched control rats. Control values at each time point were considered as 1.0. The histograms in each of the panels are the mean  $\pm$  S.E.M., n = 5. \*Significantly different from the control group at the same time point; #significantly different from 6- and 12-week time points.

cantly larger compared to the cells lining typical intralobular ducts and ductules described above as components of E<sub>2</sub>-induced lobular hyperplasia. These atypical cells were cuboidal to low columnar with an increased cytoplasmic-to-nuclear ratio when compared to categorically similar ducts described above as a component of E<sub>2</sub>-induced lobular hyperplasia. The cytoplasm was clear to amphophilic to eosinophilic and sometimes manifested microvacuolization. Nuclei were round to oval with finely stippled chromatin and often contained prominent multiple nucleoli. Mitotic figures were present, but infrequent.

At 18 weeks lobular involution was evident in all mammary glands examined. The lobular involution was characterized by depletion and degeneration of both typical normal appearing alveoli and intralobular ducts and ductules resulting in a decreased density of glands per unit area of tissue (data not shown). Ductular lumens had an increased number of sloughed degenerated epithelial cells present in amphophilic secretion. Residual alveolar and ductal epithelium contained cytoplasmic vacuoles, brown granular lipofuscin, and occasional apoptotic bodies. Both atypical alveolar and ductal hyperplasia had progressed in severity by 18 weeks.

**DNA methylation changes during E<sub>2</sub>-induced mammary carcinogenesis.** To investigate the role of epigenetic changes during

E<sub>2</sub>-induced mammary gland carcinogenesis, we first analyzed alterations in the DNA methylation profile in breast tissue after 6-, 12-, and 18-week E<sub>2</sub>-treatment using a sensitive HpaII-based cytosine extension assay that measures the proportion of unmethylated CCGG sites. The assay is based on the ability of the methylation-sensitive restriction enzyme HpaII to cleave the unmethylated sequences and leave a 5' guanine overhang that can be used for a subsequent single nucleotide extension with labeled [<sup>3</sup>H]dCTP.<sup>35</sup> The extent of [<sup>3</sup>H]dCTP incorporation is directly proportional to the number of unmethylated CCGG sites. At each sampling interval, there was a significant increase (1.20–1.27-fold) in the incorporation of [<sup>3</sup>H]dCTP into HpaII-digested DNA isolated from the mammary tissue of E<sub>2</sub>-treated rats (Fig. 2A), which indicated an increase in DNA hypomethylation.

A recent study has shown that the methylation pattern of mammalian genome consists of short unmethylated domains (<4 kb) embedded within a matrix of long methylated domains of large repetitive DNA sequences.<sup>39</sup> Additionally, it has been suggested that genome-wide DNA hypomethylation in cancer cells is associated mainly with these repetitive elements.<sup>40</sup> In view of this, we measured the methylation status of LINE-1 elements, which constitute approximately 23% of the rat genome. Figure 2B shows the extent of

methylation in the LINE-1 elements as determined by the COBRA assay. In control rats, the ratio of undigested to BstUI-digested PCR products did not differ at any of the time points. In E<sub>2</sub>-treated rats, there was a significant increase in the ratio at 18 weeks compared to 6 and 12 weeks, indicating a decrease in LINE-1 methylation.

DNA methyltransferase 1 (DNMT1) is the main cellular enzyme responsible for maintaining DNA methylation patterns in somatic mammalian cells. Therefore, we assessed whether or not the E<sub>2</sub>-induced changes in DNA methylation were associated with an altered level of DNMT1 protein. Considering the well established link between expression of DNA methyltransferases and DNA replication,<sup>41</sup> and the fact that the E<sub>2</sub>-exposure increased cell proliferation in mammary gland (Fig. 1), to determine precisely the E<sub>2</sub>-induced changes in DNMT1 expression, we normalized the protein level of DNMT1 to the expression of proliferating cells nuclear antigen (PCNA). Figure 2C shows that the long-term exposure of ACI rats to E<sub>2</sub> resulted in the sustained decrease in DNMT1/PCNA ratio beginning after 6 and 12 weeks of E<sub>2</sub>-exposure, which may be one of the contributing factors to DNA hypomethylation. However, at later time-interval (18 weeks) the DNMT1/PCNA ratio in mammary glands of E<sub>2</sub>-treated rats increased compared to 6 and 12 week values, but still remained lower than the control values.

**Methylation of histone H3 lysine 9 and histone H4 lysine 20 and expression of Suv39h1 histone methyltransferase during E<sub>2</sub>-induced mammary carcinogenesis.** Recent studies have indicated that the global loss of DNA methylation may be associated with alterations in the methylation of histones, specifically with a decreased trimethylation of H4 lysine 20 (H4K20me3).<sup>18</sup> The combined loss of DNA methylation and histone H4K20me3 was reported to be an indicator of tumorigenic process.<sup>18</sup> In view of this, we investigated the interrelationship between changes of DNA methylation and histone H3 and H4 trimethylation during mammary gland carcinogenesis.

Figure 3A shows the changes in histone H3K9me3 and H4K20me3 in the mammary glands of ACI rats exposed to E<sub>2</sub> and in their age-matched control rats. Because of the considerable E<sub>2</sub>-induced proliferative activity in mammary tissue (Figs. 1 and 2C) and the fact that histone levels are associated with cell proliferation, we normalized the changes in H3K9me3 and H4K20me3 to the level of histone H3 and histone H4, respectively. Exposure of ACI rats to E<sub>2</sub> resulted in a rapid and sustained loss of H3K9me3 and H4K20me3 in breast tissue. In contrast, exposure of ACI rats to E<sub>2</sub> was characterized by a prominent increase in histone methyltransferase Suv39h1 level in mammary glands of E<sub>2</sub>-treated rats (Fig. 3B), while the expression of Suv4-20h2 did not change significantly (data not shown).

**Aurora-A kinase expression during E<sub>2</sub>-induced mammary carcinogenesis.** The observed global DNA and LINE-1 hypomethylation and loss of histone H3K9 and H4K20 trimethylation may, in turn, severely impact heterochromatin organization predisposing the cells to genomic instability and neoplastic cell transformation. To determine whether or not the observed epigenetic alterations in the mammary tissue of E<sub>2</sub>-treated rats were associated with increased genome destabilization, we measured the expression of Aurora-A kinase, which plays a crucial role in chromosomal stability.<sup>42</sup> The levels of Aurora-A kinase protein did not change after 6 and 12 weeks of E<sub>2</sub>-exposure when compared to the age-matched control rats (Fig. 3C). However, a significant increase in Aurora-A kinase protein level was detected after 18 week of E<sub>2</sub>-treatment. This finding corresponds to the recent observation by Li et al.<sup>34</sup> showing a high level

of Aurora-A kinase mRNA and protein in mammary glands of ACI rats after four months of E<sub>2</sub>-exposure.

**miRNA gene expression changes during E<sub>2</sub>-induced mammary carcinogenesis.** Epigenetic changes in the E<sub>2</sub>-exposed mammary glands were accompanied by the profound alterations in cellular proliferation and transformation. Considering recent findings indicating the crucial role of microRNAs in the regulation of various cellular processes, such as differentiation, proliferation, and apoptosis,<sup>20,21</sup> we analyzed the expression of miRNAs during E<sub>2</sub>-induced breast carcinogenesis. Cluster analysis revealed a significant change in the miRNAome profiles in the E<sub>2</sub>-treated rats (Table 1). After 6 and 12 weeks of E<sub>2</sub> exposure, 15 miRNAs were down-regulated and 19 miRNAs were up-regulated; whereas, after 18 weeks of E<sub>2</sub> treatment, only 1 miRNA was down-regulated and 5 miRNAs were upregulated. The difference between the 6- and 12-week samples and the 18-week samples may be due to the fact that by 18 weeks of E<sub>2</sub> treatment, the mammary glands were characterized by the lobular involution of hyperplasia, a lesion that was not presented after 6 and 12 weeks.

The results obtained by miRNA microarray analysis for the samples at 6 and 12 weeks were independently confirmed by qRT-PCR, by measuring the expression of *miR-17-5p*, *miR-20a*, *miR-21*, *miR-22*, *miR-92*, *miR-106a*, *miR-127* and *miR-129-3p* miRNA genes in mammary glands of E<sub>2</sub>-treated and age-matched control rats (Table 2). In view of the fact that miRNAs negatively regulate their gene targets and the biological significance of miRNA deregulation depends on their protein-coding gene targets, we analyzed the protein levels of the experimentally confirmed targets of the differentially regulated miRNAs in mammary glands after 12 week of E<sub>2</sub>-exposure. Figure 4 shows the level of proteins targeted by miR-17-5p (E2F1),<sup>43</sup> miR-20a (E2F1),<sup>43,44</sup> miR-106a (RB1)<sup>45</sup> and miR-127 (BCL6)<sup>23</sup> in mammary glands of rats exposed to E<sub>2</sub> and control rats. The levels of RB1 and E2F1 proteins in mammary glands of E<sub>2</sub>-treated rats were decreased by 39% and 74%, respectively, compared to the age-matched control rats, which was associated with an up-regulation of miR-17-5p, miR-18, miR-20a, miR-92, and miR-106 miRNAs (Tables 1 and 2). In contrast, level of the BCL6 protein in mammary glands of rats exposed to E<sub>2</sub> was 38% greater than in the control group. Additionally, considering the fact that transcription of *miR-17-92* cluster is directly activated by c-Myc,<sup>43</sup> we measured the level of c-Myc protein in mammary glands of E<sub>2</sub>-exposed rats. The level of c-Myc protein was increased by 44% compared to control rats (Fig. 4).

## DISCUSSION

In this study, we analyzed the morphological changes and alterations that occurred during early stages of estrogen-induced breast carcinogenesis in three components of cellular epigenome. Female ACI rats provide a physiologically relevant and genetically defined animal model for studying human sporadic breast cancer as they share many relevant histopathologic and molecular features in both early pre-malignant lesions and primary tumors.<sup>33,34</sup>

The temporal shift in the morphological pattern of E<sub>2</sub>-induced mammary gland growth from a diffuse typical or normal appearing ductular and alveolar hyperplasia to focal hyperplastic areas composed of atypical appearing glands and ducts suggests clonal expansion of epithelial cells with aberrant growth. Consistent with this hypothesis is the increased cytoplasmic basophilia present in the atypical alveolar epithelial cells, implicating up-regulation of cytoplasmic RNA and

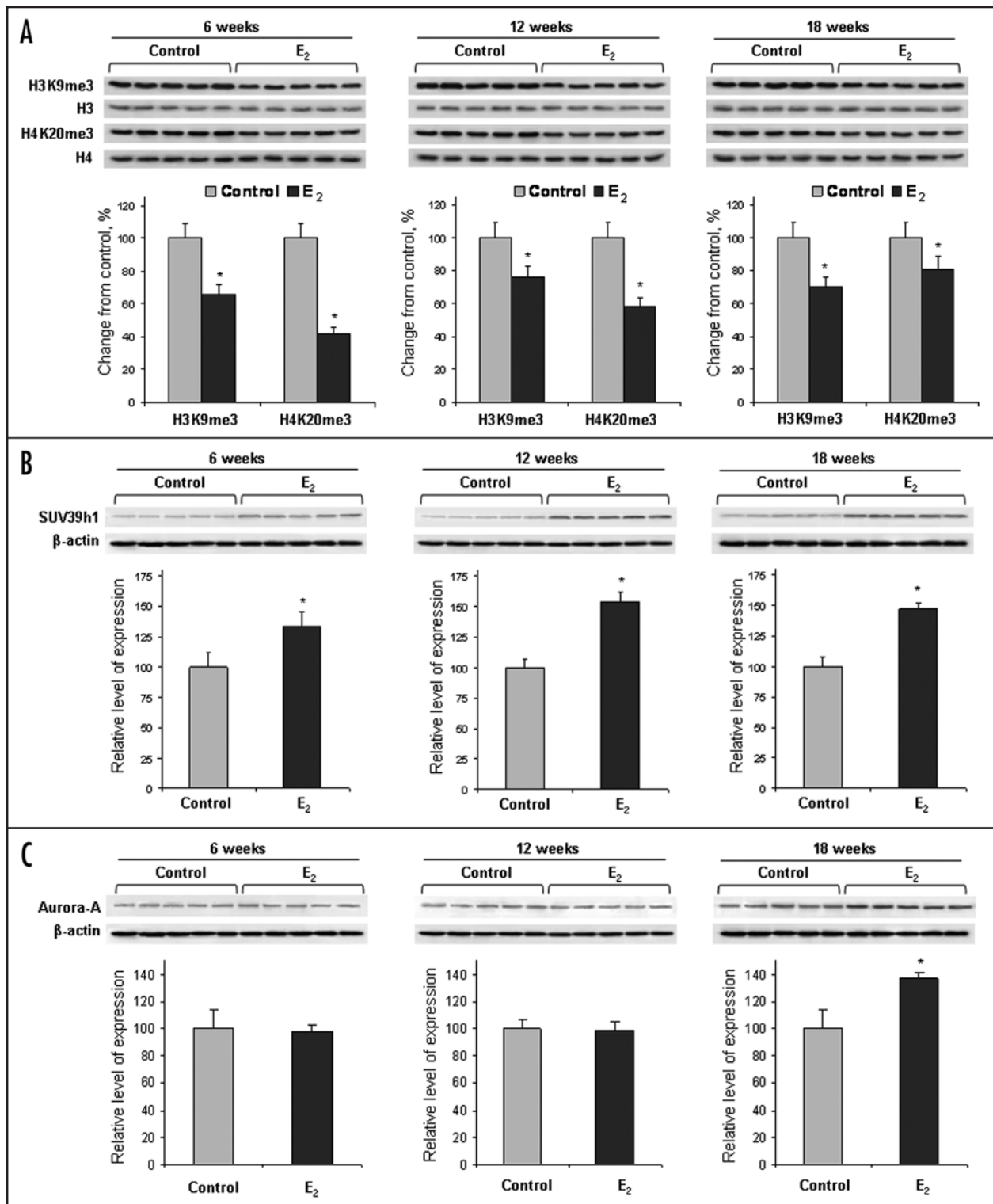


Figure 3. Western blot analysis of histone H4K20me3 and H3K9me3 and expression of histone methyltransferase Suv39h1 and Aurora-A kinase in mammary glands of control rats and rats exposed to E<sub>2</sub>. (A) Western blot analysis of histone H4K20me3 and H3K9me3. Acid extracts of total histones were separated by SDS-PAGE and subjected to immunoblotting using specific antibodies against histone H4K20me3 and H3K9me3. Equal sample loading was confirmed by immunostaining against histone H3 and histone H4. The upper part of the panel shows representative Western immunoblot images from two independent experiments. The lower part of the panel shows a quantitative evaluation of the H3K9me3 and H4K20me3 in mammary glands of E<sub>2</sub>-exposed ACI rats relative to those of control animals. (B) Western blot analysis of Suv39h1 expression. Mammary tissue lysates were separated by SDS-PAGE and subjected to immunoblotting using specific antibodies against Suv39h1 and Suv4-20h2. Equal sample loading was confirmed by immunostaining against  $\beta$ -actin. The upper part of the panel shows representative Western immunoblot images from two independent experiments. The lower part of the panel shows a quantitative evaluation of the Suv39h1 expression in E<sub>2</sub>-exposed ACI rats relative to those of control animals. (C) Western blot analysis of the Aurora-A kinase expression. Data are presented as percent fractions of controls (mean  $\pm$  S.E.M., n = 5). Control values at each time point were considered as 100%. \*Significantly different from the control group at the same time point.

**Table 1 Differentially expressed miRNA genes in mammary glands of female ACI rats exposed to E<sub>2</sub> for 6, 12, or 18 weeks<sup>a</sup>**

miRNA	Downregulated			miRNA	Upregulated		
	Weeks of E <sub>2</sub> Exposure				Weeks of E <sub>2</sub> Exposure		
	6	12	18		6	12	18
rno-miR-22*	-3.4	-3.1		rno-miR-20b	2.7	2.7	
rno-miR-99a	-2.6	-2.0		rno-miR-363-3p	2.9	2.9	
rno-miR-127	-8.4	-4.4		mmu-miR-17-5p	2.5	2.2	
rno-miR-499	-2.3	-1.9		mmu-miR-18	3.1	2.7	
mmu-miR-29c	-1.8	-1.5		mmu-miR-20a	2.5	2.3	
mmu-miR-99b	-1.4	-1.4		mmu-miR-21		1.9	1.8
mmu-miR-100	-2.5	-1.9		mmu-miR-25	2.4	1.8	
mmu-miR-139		-2.3	-1.6	mmu-miR-92	2.6	2.0	
mmu-miR-149	-2.4	-1.9		mmu-miR-93	1.9	1.6	
mmu-miR-151	-1.5	-1.7		mmu-miR-103	1.6	1.4	1.2
mmu-miR-196a	-2.2	-6.3		mmu-miR-106a	2.5	2.2	
mmu-miR-335	-6.7	-7.2		mmu-miR-106b	1.9	1.6	
mmu-miR-338	-19.4	-3.7		mmu-miR-107	1.5	1.4	1.2
mmu-miR-365	-2.3	-2.7		mmu-miR-129-3p	58.0	12.2	20.3
mmu-miR-539	-6.1	-6.4		mmu-miR-148a	1.6	1.5	1.9
mmu-let-7e	-1.2	-1.1		mmu-miR-181a	2.1	1.5	
				mmu-miR-181b	1.9	1.5	
				mmu-miR-290	3.4	3.4	
				mmu-miR-363	3.3	3.3	
				mmu-miR-375	8.9	15.7	

<sup>a</sup>miRNAs were analyzed as described in Materials and Methods. The data are presented as the fold change (decrease or increase) compared to the age-matched control group. Only values that were significantly ( $p < 0.05$ ) decreased or increased are shown.

**Table 2 qRT-PCR analysis of miR-17-5p, miR-20a, miR-92, miR-21, miR-129-3p, miR-106a, miR-22, and miR-127 in mammary glands of E<sub>2</sub>-treated rats**

miRNA	Fold Induction			Confirmed Targets
	6 Weeks	12 Weeks	18 Weeks	
mmu-miR-17-5p	4.5	1.4	-	E2F1
mmu-miR-20a	2.1	1.8	-	E2F1, E2F3
mmu-miR-92	2.0	1.5	-	E2F1
mmu-miR-21	-	1.5	2.3	TPM1, BCL2
mmu-miR-129-3p	4.0	3.0	7.8	E2F3 *
mmu-miR-106a	2.2	1.4	-	RB1
rno-miR-22	-1.5	-2.2	-	
rno-miR-127	-4.1	-7.3	-	BCL6

<sup>a</sup> The data are presented as average fold change of the signal ratios of each miRNA normalized to that of 5S rRNA of E<sub>2</sub>-treated rats compared to control rats. These values represent the mean of five biological replicates. \* Predicted target ([www.targetscan.org](http://www.targetscan.org))

probably protein synthesis. The regression and depletion of both alveoli and ducts (lobular involution) observed at 18 weeks was in sharp contrast to the significant lobular hyperplasia in the mammary gland that was present in rats at 12 weeks after the initiation of E<sub>2</sub> exposure. This may be due to the fact that the implanted E<sub>2</sub> pellet

was estimated to last 90 days. By 18 weeks (126 days), the E<sub>2</sub> had likely been depleted, possibly resulting in the arrest of hormone-induced mammary gland growth stimulus. The marginal decrease in atypical alveolar hyperplasia that occurred at 18 weeks was in the same time frame as involution suggesting that the formation and progressive growth of atypical alveolar foci were up-regulated by E<sub>2</sub>, and, after the depletion of E<sub>2</sub>, at least some of these atypical foci may have undergone involution along with the obvious regression of typical normal appearing alveoli and ducts. This interpretation is supported by mild degenerative changes that were present in some of the residual atypical foci. Interestingly, in the rats that retained alveolar atypical hyperplastic foci in the mammary gland at 18 weeks. Moreover, the prevalence of atypical ductal hyperplasia remained at 100% and progressively increased for the group of E<sub>2</sub>-treated rats at 18 weeks. These results suggest two possibilities: (1) that the regression of atypical hyperplastic lesions, after discontinuation of E<sub>2</sub> treatment, lagged behind involution of typical lobular hyperplasia of the mammary gland or (2) some atypical foci no longer required E<sub>2</sub> stimulation for

maintenance and/or support of further growth. Additional studies will be needed to examine these possibilities.

The results of this study show that deregulation of cellular epigenetic processes plays a crucial role in the mechanism of E<sub>2</sub>-induced mammary carcinogenesis in ACI rats, especially in the tumor initiation process. This was evidenced by a rapid and sustained loss of global DNA methylation, which was accompanied by a decrease in the levels of H3K9me3 and H4K20me3. More importantly, these epigenetic alterations in the mammary tissue occurred after 6 weeks of E<sub>2</sub>-treatment, whereas the atypical hyperplasia, which represents a putative precursor lesion to mammary carcinoma in this model,<sup>33,34</sup> was only detected after 12 weeks of exposure, demonstrating clearly that these events are directly associated with the effects of E<sub>2</sub> and are not a consequence of the preexisting preneoplastic lesions. Several possible mechanisms can be proposed for the loss of DNA and histone methylation, such as estrogen-induced DNA damage, increased cell proliferation, altered expression of DNA methyltransferases, and interference or influence of preexisting modifications in the amino-terminal tails of histones H3 and H4. Any or all of these mechanisms may also affect stability of the genome leading to neoplastic cell transformation.

In order to determine whether the observed epigenetic changes are mechanistically related to genome destabilization and neoplastic cell transformation, we measured the Aurora-A kinase protein level. Recent studies have implicated over-expression of centrosome-associated kinase Aurora-A with chromosomal instability<sup>42</sup> and have suggested that the high levels of Aurora-A may be a crucial event

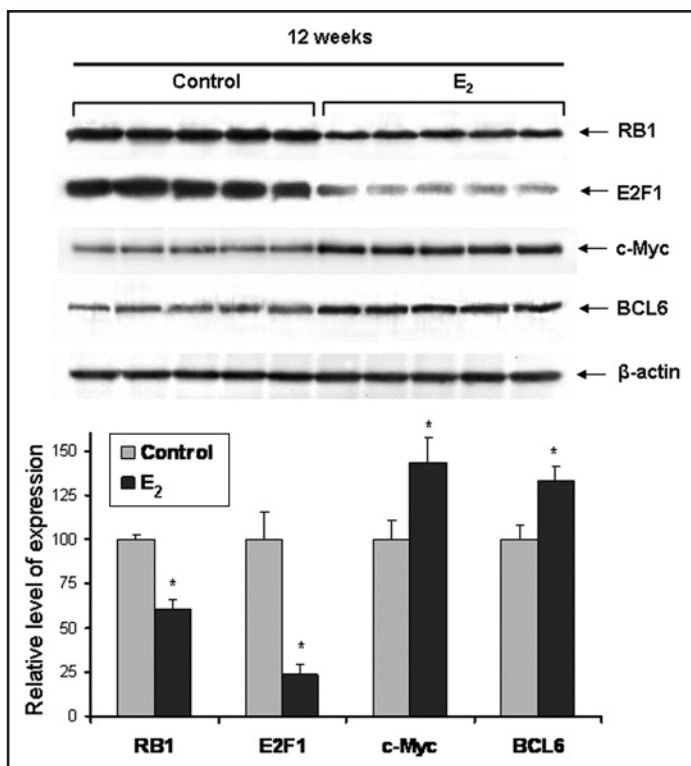


Figure 4. Western blot analysis of the RB1, E2F1, c-Myc and BCL6 proteins in mammary glands of control rats and rats exposed to E<sub>2</sub>. Mammary tissue lysates were separated by SDS-PAGE and subjected to immunoblotting using specific antibodies against RB1, E2F1, c-Myc and BCL6 proteins. Equal sample loading was confirmed by immunostaining against  $\beta$ -actin. The upper part of the figure shows representative Western immunoblot images from two independent experiments. The lower part of the figure shows a quantitative evaluation of the RB1, E2F1, c-Myc and BCL6 proteins in E<sub>2</sub>-exposed ACI relative to those of control animals. Data are presented as relative to age-matched control rats after normalization to  $\beta$ -actin (mean  $\pm$  S.E.M., n = 5). Control values were considered as 100%. \* - Significantly different from the control group.

during early mammary gland tumor development.<sup>34</sup> Our data demonstrated the increased level of Aurora-A in the mammary tissue of ACI rats after 18 weeks of E<sub>2</sub>-treatment, 6 weeks after the first appearance of atypical hyperplasia, a precursor lesion to mammary gland tumors. A comparison of the dynamic changes in Aurora-A expression with morphological changes in the mammary gland clearly demonstrates that over-expression of Aurora-A is associated with the progression of the neoplastic process rather than the initiation of malignancy.

The changes in miRNAs expression in the rat mammary glands induced by E<sub>2</sub>-exposure constitute a novel and important outcome of this study. miRNAs are small non-coding RNAs that function as key negative regulators of gene expression.<sup>20,21</sup> Additionally, they have been proposed to be regulators of epigenetic status and chromatin structure.<sup>22</sup> Alternatively, recent evidence has indicated that some miRNAs are controlled by epigenetic mechanisms.<sup>23,24</sup> Aberrant levels of miRNAs have been reported in a variety of human cancers,<sup>25,26</sup> including breast cancer.<sup>27</sup> This observation suggested that deregulation of miRNAs expression may play an important role in the pathogenesis of human tumors.<sup>25-27</sup> However the dynamics of miRNA changes during pre-malignant stages have not been studied. Here we show for the first time that miRNA alterations, specifically

expression changes of known oncogenic miRNAs precede tumor formation. For instance, miR17-5p and miR-106a from miR-17-92 cluster, which target the important cell cycle regulators E2F1 and RB1,<sup>43-45</sup> were up-regulated. It is believed that oncogenic aspect of miR-17-92 cluster is due, in part, to a reduced apoptotic program.<sup>44</sup> Indeed, down-regulation of the RB1 and E2F1 may lead to deregulated expression of the RB/E2F1 down-stream targets, such as PCNA, cyclin A, cyclin E, and other proteins involved in cell cycle control favoring cell proliferation over apoptosis. A strong up-regulation of PCNA and c-Myc in the mammary glands of rats exposed to E<sub>2</sub> (Figs. 2C and 4) support this suggestion. In addition, a direct role of c-Myc in activation of miR-17-92 cluster has been shown recently.<sup>43</sup> In light of these considerations, and the crucial role of c-Myc in the development of breast tumors,<sup>46</sup> the ability of c-Myc to promote mammary gland tumorigenesis by driving unrestricted cell proliferation may be related to its role in activation of miR-17-92 cluster. Additionally, considering a major role of RB1 in the assembly of constitutive heterochromatin by maintaining the histone H4 lysine 20 trimethylation state,<sup>47</sup> loss of RB1 may further contribute to the loss of histone H4 lysine 20 trimethylation and compromise the heterochromatin organization in cells. We also detected an increased level of expression of miR-20a and miR-21. miR-20a targets transforming growth factor  $\beta$  receptor II,<sup>45</sup> the inactivation of which results in malignant transformation,<sup>48</sup> and the over-expression of miR-21 frequently observed in human breast tumors.<sup>49</sup>

Amongst the down-regulated miRNAs were miR-22, miR-99a, miR-99b, and miR-127. Recent evidence has indicated that miR-127 may act as tumor suppressor by targeting the BCL-6 proto-oncogene;<sup>23</sup> as such, the decreased expression of miR-127, induced by treatment with E<sub>2</sub>, may promote neoplastic cell transformation. These changes in expression of miRNA genes on one hand may be implicated in affecting cell proliferation, apoptosis, and transformation, while on other hand they may contribute to maintenance and regulation cellular epigenome. Moreover, these changes occur early and are similar to previously reported alterations in human breast tumors.<sup>27,49,50</sup> Indeed, the profound changes in the levels of miR-21, miR-25, miR-99a, miR-99b, miR-106a, miR-106b, and let-7 were reported to occur in full-fledged human breast tumors.<sup>27,50</sup>

Importantly, we have shown for the first time a significant correlation between the appearances of changes in the three main components of epigenetics. As mentioned above, there is a major gap in our understanding of the role of epigenetic dysregulation in carcinogenesis, particularly a lack of knowledge about specific epigenetic changes that may be mechanistically related to neoplastic transformation, and the precise timeline of epigenetic alterations occurring in the transition of a normal cell to a tumor cell.<sup>28,29</sup> By comparing the emergence of epigenetic alterations with the observed morphological changes in mammary tissue, we were able to provide evidence that epigenetic changes precede formation of preneoplastic lesions.

The epigenetic dysregulation observed in this study occurred in the context of the activation of pro-survival growth-stimulatory cellular signaling pathways. Changes in DNA and histone methylation, and, importantly, deregulation in the miRNAome may lead to the emergence of epigenetically reprogrammed cells with a tumor-specific phenotype (inhibition of cell cycle arrest and apoptosis, activation of cell proliferation) leading to subsequent malignant transformation.

## References

- Schairer C, Mink PJ, Carroll L, Devesa SS. Probabilities of death from breast cancer and other causes among female breast cancer patients. *J Natl Cancer Inst* 2004; 96:1311-21.
- Raval R, Bermejo JL, Hemminki K. Risk of subsequent invasive breast carcinoma after in situ breast carcinoma in a population covered by national mammographic screening. *Br J Cancer* 2005; 92:162-6.
- Simpson PT, Reis-Filho JS, Cale T, Lakhani SR. Molecular evolution of breast cancer. *J Pathol* 2005; 205:248-54.
- Ellsworth DL, Ellsworth RE, Liebman MN, Hooke JA, Shriver CD. Genomic instability in histologically normal breast tissues: Implications for carcinogenesis. *Lancet Oncol* 2004; 5:753-8.
- Egger G, Liang G, Aparicio A, Jones PA. **Epigenetics in human disease and prospects for epigenetic therapy.** *Nature* 2004; 429:457-63.
- Widschwendter M, Jones PA. DNA methylation and breast carcinogenesis. *Oncogene* 2002; 21:5462-82.
- Feinberg AP, Tycko B. The history of cancer epigenetics. *Nature Rev Cancer* 2004; 4:143-5.
- Jones PA, Baylin SB. The epigenomics of cancer. *Cell* 2007; 128:683-92.
- Feinberg AP, Vogelstein B. Hypomethylation distinguishes genes of some human cancers from their normal counterparts. *Nature* 1983; 301:89-92.
- Flatau E, Bogenmann E, Jones PA. **Variable 5-methylcytosine levels in human tumor cell lines and fresh pediatric tumor explants.** *Cancer Res* 1983; 43:4901-5.
- Gama-Sosa MA, Slagel VA, Trewyn RW, Oxenhandler R, Kuo KC, Gehrke CW, Ehrlich M. The 5-methylcytosine content of DNA from human tumors. *Nucl Acid Res* 1983; 11:6883-94.
- Hsieh CL, Jones PA. **Meddling with methylation.** *Nature Cell Biol* 2003; 5:502-4.
- Narayan A, Ji W, Zhang XY, Marrogi A, Graff JR, Baylin SB, Ehrlich M. Hypomethylation of pericentromeric DNA in breast adenocarcinomas. *Int J Cancer* 1998; 77:833-8.
- Soares J, Pinto AE, Cunha CV, André S, Barão I, Sousa JM, Cravo M. Global DNA hypomethylation in breast carcinoma: correlation with prognostic factors and tumor progression. *Cancer* 1999; 85:112-8.
- Tsuda H, Takarabe T, Kanai Y, Fukutomi T, Hirohashi S. Correlation of DNA hypomethylation at pericentromeric heterochromatin regions of chromosomes 16 and 1 with histological features and chromosomal abnormalities of human breast carcinomas. *Am J Pathology* 2002; 161:859-66.
- Robertson KD. DNA methylation and chromatin -unraveling the tangled web. *Oncogene* 2000; 21:5361-79.
- Hake SB, Xiao A, Allis CD. Linking epigenetic 'language' of covalent histone modifications to cancer. *Br J of Cancer* 2004; 90:761-9.
- Fraga MF, Ballestar E, Villar-Garea A, Boix-Chornet M, Espada J, Schotta G, Bonaldi T, Haydon C, Ropero S, Petrie K, Iyer NG, Pérez-Rosado A, Calvo E, Lopez JA, Cano A, Calasanz MJ, Colomer D, Piris MA, Ahn N, Imhof A, Caldas C, Jenuwein T, Esteller M. Loss of acetylation at Lys 16 and trimethylation of histone H4 is a common hallmark of human cancer. *Nature Genet* 2005; 37:391-400.
- Santos-Rosa H, Caldas C. Chromatin modifier enzymes, the histone code and cancer. *Eur J Cancer* 2005; 41:2381-402.
- Sevignani C, Calin GA, Siracusa LD, Croce CM. Mammalian microRNAs: A small world for fine-tuning gene expression. *Mamm Genome* 2006; 3:189-06.
- Carthew RW. Gene regulation by microRNAs. *Curr Opin Genet Devel* 2006; 16:203-8.
- Bernstein E, Allis CD. RNA meets chromatin. *Genes Devel* 2006; 19:1635-55.
- Saito Y, Liang G, Egger G, Friedman JM, Chuang JC, Coetzee GA, Jones PA. Specific activation of microRNA-127 with down regulation of the proto-oncogene *BCL6* by chromatin-modifying drugs in human cancer cells. *Cancer Cell* 2006; 9:435-43.
- Lujambio A, Ropero S, Ballestar E, Fraga MF, Cerrato C, Setien F, Casado S, Suarez-Gauthier A, Sanchez-Cespedes M, Git A, Spiteri I, Das PP, Caldas C, Miska E, Esteller M. Genetic unmasking of an epigenetically silenced microRNA in human cancer cells. *Cancer Res* 2007; 67:1424-9.
- Lu J, Getz G, Miska EA, Alvarez-Saavedra E, Lamb J, Peck D, Sweet-Cordero A, Ebert BL, Mak RH, Ferrando AA, Downing JR, Jacks T, Horvitz HR, Golub TR. MicroRNA expression profiles classify human cancers. *Nature* 2005; 435:834-8.
- Calin GA, Croce CM. MicroRNA-cancer connection: The beginning of a new tale. *Cancer Res* 2006; 66:7390-4.
- Iorio MI, Ferracin M, Liu CG, Veronese A, Spizzo R, Sabbioni S, Magri E, Pedriali M, Fabbri M, Campiglio M, Ménard S, Palazzo JP, Rosenberg A, Musiani P, Volinia S, Nenci I, Calin GA, Querzoli P, Negrini M, Croce CM. MicroRNA gene expression deregulation in human breast cancer. *Cancer Res* 2005; 65:7065-70.
- Baylin S, Bestor TH. Altered methylation patterns in cancer genomes: Cause or consequence? *Cancer Cell* 2002; 1:299-305.
- Ushijima T, Okochi-Takada E. Aberrant methylations in cancer cells: Where do they come from? *Cancer Sci* 2005; 96:206-11.
- Ye Y, Qiu TH, Kavanaugh C, Green JE. Molecular mechanisms of breast cancer progression: Lessons from mouse mammary cancer models and gene expression profiling. *Breast Disease* 2004; 19:69-82.
- Yager JD, Davidson NE. Estrogen carcinogenesis in breast cancer. *New Engl J Med* 2006; 354:270-82.
- Russo J, Russo IH. The role of estrogen in the initiation of breast cancer. *J Steroid Biochem Mol Biol* 2006; 102:89-96.
- Shull JD, Spady TJ, Snyder MC, Johansson SL, Pennington KL. Ovary-intact, but not ovariectomized female ACI rats treated with 17 $\beta$ -estradiol rapidly develop mammary carcinoma. *Carcinogenesis* 1997; 18:1595-601.
- Li JJ, Weroha SJ, Lingle WL, Papa D, Salisbury JL, Li SA. Estrogen mediates Aurora-A overexpression, centrosome amplification, chromosomal instability, and breast cancer in female ACI rats. *Proc Natl Acad Sci USA* 2004; 101:18123-8.
- Pogribny IP, Yi P, James SJ. A sensitive new method for rapid detection of abnormal methylation patterns in global DNA and within CpG islands. *Biochem Biophys Res Commun* 1999; 262:624-8.
- Asada K, Kotake Y, Asada R, Saunders D, Broyles RH, Towner RA, Fukui H, Floyd RA. LINE-1 hypomethylation in a choline-deficiency induced liver cancer: Dependence on feeding period. *J Biomed Biotech* 2006; 2006:17142.
- Bolstad BM, Irizarry RA, Astrandand M, Speed TP. A comparison of normalization methods for high density oligonucleotide array data based on variance and bias. *Bioinformatics* 2003; 19:185-93.
- Eisen MB, Spellman PT, Brown PO, Botstein D. Cluster analysis and display of genome-wide expression patterns. *Proc Natl Acad Sci USA* 1998; 95:14863-8.
- Rollins RA, Haghghi F, Edwards JR, Das R, Zhang MQ, Ju J, Bestor TH. Large-scale structure of genomic methylation patterns. *Genome Res* 2006; 16:157-63.
- Yoder JA, Walsh CP, Bestor TH. Cytosine methylation and the ecology of intragenomic parasites. *Trends Genet* 1997; 13:376-8.
- Vertino PM, Sekowski JA, Coll JM, Applegren N, Han S, Hickey RJ, Malkas LH. DNMT1 is a component of a multiprotein DNA replication complex. *Cell Cycle* 2002; 1:416-23.
- Marumoto T, Zhang D, Saya H. Aurora-A - A guardian of poles. *Nat Rev Cancer* 2005; 5:42-50.
- O'Donnell KA, Wentzel EA, Zeller KI, Dang CV, Mendell JT. c-Myc-regulated microRNAs modulate E2F1 expression. *Nature* 2005; 435:839-43.
- Woods K, Thomson JM, Hammond SM. Direct regulation of an oncogenic micro-RNA cluster by E2F transcription factors. *J Biol Chem* 2007; 282:2130-4.
- Volinia S, Calin G, Liu CG, Ambs S, Cimmino A, Petrocca F, Visone R, Iorio M, Roldo C, Ferracin M, Prueitt RL, Yanaihara N, Lanza G, Scarpa A, Vecchione A, Negrini M, Harris CC, Croce CM. A microRNA expression signature of human solid tumors defines cancer gene targets. *Proc Natl Acad Sci USA* 2006; 103:2257-61.
- D'Cruz CM, Guntner EJ, Boxer RB, Hartman JL, Sintasath L, Moody SE, Cox JD, Ha SI, Belka GK, Golant A, Cardiff RD, Chodosh LA. c-MYC induces mammary tumorigenesis by means of a preferred pathway involving spontaneous Kras2 mutations. *Nat Med* 2001; 7:235-9.
- Gonzalo S, Blasco MA. Role of Rb family in the epigenetic definition of chromatin. *Cell Cycle* 2005; 4:752-5.
- Seone J. Escaping from the TGF $\beta$  anti-proliferative control. *Carcinogenesis* 2006; 27:2148-56.
- Si ML, Zhu S, Wu H, Lu Z, Wu F, Mo YY. *miR-21*-mediated tumor growth. *Oncogene* 2007; 26:2799-803.
- Zhang L, Huang J, Yang N, Greshock J, Megraw MS, Giannakakis A, Liang S, Naylor TL, Barchetti A, Ward MR, Yao G, Medina A, O'Brien-Jenkins A, Katsaros D, Hatzigeorgiou A, Gimotty PA, Weber BL, Coukos G. microRNAs exhibit high frequency genomic alterations in human cancer. *Proc Natl Acad Sci USA* 2006; 103:9136-41.